PERMAFROST AND PERIGLACIAL PROCESSES
Permafrost and Periglac. Process., **22**: 179–187 (2011)
Published online 9 May 2011 in Wiley Online Library
(wileyonlinelibrary.com) DOI: 10.1002/ppp.722

Effects of Ice Content on the Thermal Erosion of Permafrost: Implications for Coastal and Fluvial Erosion

L. Dupeyrat,[1]* *F. Costard,*[1] *R. Randriamazaoro,*[1] *E. Gailhardis,*[1] *E. Gautier*[2] *and A. Fedorov*[3]

[1] UMR 8148 IDES, CNRS, Université Paris-Sud, Orsay, France
[2] Université Paris 8, CNRS, UMR 8591 Laboratoire de Géographie Physique, Meudon, France
[3] Melnikov Permafrost Institute, Russian Academy of Science, Yakutsk, Russia

ABSTRACT

The effects of ice content and water flow on thawing and erosion of non-cohesive permafrost banks were investigated through laboratory experiments. A critical ice content was identified as associated with turbulent flows (20% and 80% for Reynolds numbers of 15 900 and 12 700, respectively), above which thermal erosion results in ablation and a decrease in ice content increases ablation. Below the critical value, the ablation model over-estimates the erosion rate as the removal of thawed sediments occurs episodically, possibly due to the imbrication of sand grains. The ablation model applies to rivers with non-cohesive banks, high ice contents and subject to high-velocity water flows. The model may explain differential erosion that results in massive ice layers in relief. At other sites, however, the retreat rate increases with ground ice content. This behaviour can be explained for sandy permafrost with a relatively low ice content and heterogeneous sand sizes and shapes subject to relatively low-velocity water flow. These results apply only to perenially frozen sands, as even a small percentage of cohesive material would modify the relationships described. Copyright © 2011 John Wiley & Sons, Ltd.

KEY WORDS: Thermal erosion; thermo-erosion; thermokarst; physical modelling; ice content

BACKGROUND

Introduction

Many rivers in permafrost environments experience spectacular spring floods mainly controlled by rapid snowmelt. Water levels rapidly increase over a few days, the frozen river bank in contact with the water progressively thaws and some of the newly unfrozen sediments may be carried away by the flow, resulting in metres of bank retreat. This erosive process, caused by the thermal and mechanical energy of moving water, has been referred to as thermal erosion (Are, 1983) or fluvial thermal erosion (van Everdingen, 1998). The thermal process involves thawing of frozen sediments by turbulent water flow and once the substrate is thawed, mechanical erosion occurs if hydraulic forces exceed material strength (Gatto, 1995).

* Correspondence to: Laure Dupeyrat, UMR 8148 IDES, bât. 509, Université Paris Sud 11, 91405 Orsay Cedex, France.
E-mail: laure.dupeyrat@u-psud.fr

Thermal erosion results in thermal ablation when the thawed sediments are immediately removed by the water flow. Constant rate models (Costard *et al.*, 2003) or variable rate models of thermal ablation (Randriamazaoro *et al.*, 2007) have been developed and validated by experiments on ice samples under laboratory conditions. The relative effects of water temperature, water discharge and ice temperature have been quantified and compared revealing that water temperature is the main factor, but bank characteristics, such as ice content and sand and silt content, also affect the ablation rate.

In this paper, experiments of permafrost ablation for different ice contents are reported. In addition, a mathematical model is presented that takes into account the effects of ice content for saturated sandy permafrost. The ablation model produces very high erosion rates compared to field values, so the second objective of the study is to define experimentally the limits of validity of this model in term of hydrodynamic conditions and sediment properties. The process of thermal erosion with an accumulating thawed layer, developed when sediments are not instantaneously removed and erosion rates are lower than ablation rates, is also investigated experimentally. Finally, the application of both models to field conditions is discussed.

Received 9 February 2009
Revised 24 January 2011
Accepted 28 January 2011

Field Observations

The importance of ice content to thermal erosion rates in rivers traversing permafrost regions is well known (e.g. Are, 1983; Aguirre Puente *et al.*, 1994). Studies have focused on the erosion of frozen coastal cliffs (Gillie, 1990; Héquette and Barnes, 1990; Hoque and Pollard, 2005) and have assessed the role of ground ice contents in the formation of thermoerosional niches (e.g. Kobayashi, 1985; Kobayashi *et al.*, 1999). Aberle *et al.*'s (2004) measurements of mechanical erosion were consistent with the effect of increasing erosion rates with increasing water contents in unfrozen soils reported by Fukuda and Lick (1980).

According to Soloviev (1962), rapid mechanical removal of thawed material proceeds from river banks with 75 to 90% moisture by volume. Jepsen *et al.* (1997) and Roberts *et al.* (1998) also reported that erosion rates for homogeneous sediments increase with decreasing bulk density, which is equivalent to an increase in the moisture content of unfrozen soils. Lantuit *et al.* (2008) investigated the statistical relationship between ground ice contents and Arctic coastal erosion rates for 545 coastal segments. Their analysis revealed that retreat rates (0 to 9 m year^{-1}) increase weakly ($r = 0.4$) with volumetric ground ice content (0 to 70%) and that other factors must therefore play a role in controlling the processes. Site-specific observations in fact indicate that the opposite is sometimes the case. For instance, overhangs of massive icy beds have been observed in the eroded permafrost banks of the Lena River (Figure 1). This suggests that pure ice has been less eroded than the surrounding lower ice-content permafrost (Gautier and Costard, 2000).

These contradictory observations concerning the relation between ice contents and erosion rates show that the process is relatively complex and both its thermal and mechanical aspects require further study.

Thermal Erosion and Ice Content

The thermal influence corresponds to energy transferred to the coast or the river bank via radiative and sensible heat fluxes from the atmosphere and sensible heat from the water (Ogorodov, 2008). Heat fluxes cause displacement of the thaw front in the ground. In this study, as we are concerned with thermal erosion induced by turbulent water flow, heat fluxes from the atmosphere are neglected. The energy balance at the water/permafrost interface shows that most of this energy is used to melt the ice (i.e. to satisfy the latent heat) while a smaller portion is used to raise ground temperatures (specific heat). As the latent heat needed to thaw frozen ground increases with ice content, displacement of the thaw front is slowed for higher ice contents.

The mechanical influence corresponds to the direct impact of ocean waves on the shore, or turbulent flow on river banks. This results in the mechanical erosion of thawed sediments whose volumetric water content is almost equivalent to the volumetric ice content of the same material when frozen. Thawed sediments are generally weaker than comparable

Figure 1 Differential erosion in the Lena River bank showing overhangs of massive icy layers in permafrost. This suggests that ice-rich layers are thermally eroded more slowly than the ice-poor layers. The visible differential erosion is caused by water action during the breakup. Each year, local ice-jams and log-jams contribute to sudden rises in the water level up to 10 m, leading to rapid inundation of the first terrace (Costard and Gautier, 2007). Hydrological observations (gauging site at Tabaga and data loggers on site) clearly support such sudden variations of the flood level.

frozen materials, especially if their water content is greater than saturation (Are, 1983). After thawing, excess water contents reduce cohesion and substrate shear strength so the resistance of sediments to the water current decreases (Gatto, 1995). Experiments on reconstructed sediment samples have shown an increase in mechanical erosion as bulk density decreases (which is equivalent to a increase in water content) (Lick and McNeil, 2001).

Ogorodov (2008) suggested that the mechanical factor is more significant at low ice contents and the thermal factor becomes more important at high ice contents. Erosion rates for low ice-content coasts were correlatable with hydrometeorological data reperesenting wave energy (Ogorodov, 2008). On the other hand, the retreat of typical thermoerosional bluffs composed of sandy and clayey deposits with medium ice contents is controlled by both thermal and wave-energy factors.

In this paper, we report how ice content can influence thermal and mechanical processes. Using empirical and theoretical approaches, we demonstrate that two different processes are involved for ice-rich permafrost and low ice-content permafrost. For a sufficiently high ice content, the mechanical factor may be neglected and the process of thermal erosion results in an ablation process in which thawed sediments are immediately swept away by the water flow. This critical ice content should depend on the mechanical energy of the flow. In the case of pure ablation, the ablation rate must decrease for high ice contents because of the higher latent heat requirement.

On the other hand, below this critical ice content, some cohesion of thawed sediments must occur and the pure ablation model is no longer valid. Consequently, the increase in ice content has two opposite effects: sediment cohesion is reduced when ice content increases which enhances erosion, but displacement of the thaw front slows with an increase in ice content. Therefore, the mechanical and thermal effects of ice content on the erosion rate oppose each other for sediments without excess ice.

Erosion Processes and Sediment Type

The influence of cohesion on mechanical erosion is still unclear. In the Colville River Delta (Alaska), field measurements give an average erosion rate of less than 1 m $year^{-1}$ in cohesive peat banks, but more than 2 m $year^{-1}$ in sands and gravels (Walker, 1983). Faster erosion rates usually relate to coarser, cohesionless sediments (Scott, 1978) and the resistance of temperate river banks to fluvial erosion increases with cohesion (Thorne and Tovey, 1981; Osman and Thorne, 1988; Couper, 2003). The erodibility of cohesive bank material is a function of a complex combination of physico-chemical and intergranular forces that control the resistance of aggregates to detachment by fluid shear. No complete theory for the erosion of cohesive banks exists (Lawler *et al.*, 1997).

Non-cohesive material is usually detached and entrained grain by grain and the stability of the substrate depends on the balance of fluid force, gravity force, and the resisting forces of friction and interlocking (Lawler *et al.*, 1997). The fluid forces can be represented by boundary shear stress. The resisting forces increase with the imbrication of grains, which is favoured by non-spherical shapes and the presence of fine interstitial material (Lawler *et al.*, 1997). Measurements of mechanical erosion on various uniform-sized quartz sediments (from 5 to 1350 μm in diameter) showed that for the larger particles, the sediments behaved in a non-cohesive manner (i.e. the surface eroded particle by particle) while for the smaller particles, the sediments behaved in a cohesive manner (i.e. the surface eroded as aggregates as well as separates) (Lick and McNeil, 2001). These experiments also showed that the particle size distribution has a significant effect on erosion rate.

Model for Permafrost Thermally Eroded by Flowing Water

The literature referred to previously demonstrates that a model of thermal erosion must distinguish between cohesive and non-cohesive sediments. For the former, the pure thawing model gives a lower limit for displacement of the thaw front. In the case of non-cohesive sediments, the pure ablation model gives an upper limit for displacement of the thaw front, which is also the erosion front. As this pure ablation model may over-estimate the erosion of the ground, a general approach is needed.

Model for Saturated or Supersaturated Permafrost

Permafrost can be regarded as a saturated or 'supersaturated' porous medium with a volume of ice equal to or greater than the volume of porewater before ground freezing (Dysli, 2003). Permafrost is then a two-component medium composed of ice and mineral particles or water and mineral particles when thawed. The density (Equation 1), as well as the specific heat (Equation 2) and latent heat (Equation 3) of a soil can be obtained from those of the components and the ice content ($\omega = m_{ice}/m_s$).

$$\rho_{sat} = \frac{\rho_{ice}\rho_s(\omega + 1)}{\rho_s\omega + \rho_{ice}} \quad (1)$$

$$Cp_{sat} = \left(\frac{\omega}{1+\omega}\right).Cp_{ice} + \left(\frac{1}{1+\omega}\right).Cp_s \quad (2)$$

$$L_{sat} = \left(\frac{\omega}{1+\omega}\right).L_{ice} \quad (3)$$

where ρ [$kg.m^{-3}$] is the density, cp [$J.kg^{-1}.°C^{-1}$] is the specific heat, L [$J.kg^{-1}$] is the latent heat of fusion, ω [%] is the massic ice content of permafrost, and the subscripts $_{ice}$ and $_s$ refer to ice and sediment particles, respectively.

The thermal conductivity of a soil depends on the thermal properties and volume fraction of the different components

as well as on microstructural parameters, such as geometry of the pore structure and size distribution of the mineral solids. Numerous purely empirical, semi-empirical or theoretical methods have been developed for calculating the thermal conductivity of soils. In the case of saturated soils, Johansen (1975) found that microstructure had little effect on thermal conductivity. For a saturated soil, the Johansen method (Equation 4) gives good agreement with measured values (Farouki, 1981).

$$k_{sat} = k_{ice}{}^{n}.k_s{}^{(1-n)} \quad (4)$$

where k_{ice} and k_s [$W.m^{-1}.°K^{-1}$] are the thermal conductivity of ice and the solid phase, respectively, and n [dimensionless] is the fractional porosity.

n is related to the ice content (ω) by:

$$n = \frac{1}{1 + \left(\frac{\rho ice}{\rho s.\omega}\right)} \quad (5)$$

For unfrozen soils, the same formulations are valid if the ice characteristics are replaced by the characteristics of water.

Model of Pure Thaw (without Ablation) for Cohesive Permafrost

In the pure thaw model, it is assumed that thawed sediments, which are highly cohesive, are not removed at all by the flow. As a result, an approximate solution of the Stefan problem can be used, with convective flux at the water/permafrost boundary. Assuming a linear temperature profile in the thawed sediments, the position of the thaw front is obtained from (Aguirre Puente *et al.*, 1994):

$$s(t) = -\frac{k_{tha}}{h} + \sqrt{\left[\left(\frac{k_{tha}}{h}\right)^2 + 2.\frac{k_{tha}}{\rho_{per}.L_{per}}\left(T_w - T_f\right)\right].t} \quad (6)$$

where ρ_{per} [$kg.m^{-3}$] and L_{per} [$J.kg^{-1}$] are the density and latent heat of the permafrost, respectively, h [$W.m^{-2}.°C^{-1}$] is the heat transfer coefficient at the water/permafrost interface, T_w and T_f [°C] are the water temperature and thawing temperature, respectively, and k_{tha} [$W.m^{-1}.°K^{-1}$] is the thermal conductivity of the thawed sediments.

Model of Pure Ablation for Non-cohesive Permafrost

The pure ablation model (Aguirre-Puente et al., 1994; Costard *et al.*, 2003; Randriamazaoro *et al.*, 2007) assumes an instantaneous removal of thawed sediments. Initially, isothermal permafrost remains in continuous contact with a turbulent flow of isothermal warm water. These assumptions allow the resolution of conservation of energy in permafrost and heat flux balance at the water/permafrost interface to be used to calculate the water/permafrost interface position (Carslaw and Jaeger, 1959; Aguirre Puente et al., 1994):

$$s_a(t) = \frac{h.(T_w - T_f)}{\rho_{per}.\left[L_{per} - T_i.c_{p_{per}}\right]}.t \quad (7)$$

where T_i [°C], ρ_{per} [$kg.m^{-3}$] cp_{per} [$J.kg^{-1}.°C^{-1}$] and L_{per} [$J.kg^{-1}$] are the initial temperature, density, specific heat and latent heat of the permafrost, h [$W.m^{-2}.°C^{-1}$] is the heat transfer coefficient at the water/permafrost interface, and T_w and T_f [°C] are the water temperature and thaw temperature, respectively.

Model of Thermal Erosion for Non-cohesive Permafrost

Theoretically, the ablation model could be used for homogeneous non-cohesive sediments, but even banks developed in coarse materials exhibit some cohesion due to the degree of packing and imbrication of sand grains (Lawler *et al.*, 1997). Consequently, propagation of the thaw front is not constant and ablation removes a portion of the thawed sediments episodically. This makes the process difficult to model and justifies an empirical approach using laboratory simulation.

EXPERIMENTAL SETUP

The pure ablation model (Equation 7) was previously validated using ice samples in thermal contact with a hydraulic channel flume in a cold room (Costard *et al.*, 2003). In the present study, we used our hydraulic channel (Figure 2) in combination with a new method for preparing supersaturated frozen samples. Bayeux sand, which has a heterogeneous grain size distribution between 0.1 and 0.5 mm (Figure 2), was mixed with water to a dry density of 1.81 g cm^{-3}, corresponding to the Proctor compaction. Predetermined amounts of snow and ice particles less than 1 mm in diameter were then introduced into the sample to obtain an ice content of 20% or 80% by mass. The sample was then frozen.

Experiments were undertaken using frozen soil samples at temperatures from −15 °C to −2 °C, in contact with flowing water at temperatures between 5 °C and 15 °C with Reynolds numbers from 6000 to 20 000. Erosion was measured each 30 s for 20 min. For each experiment, ablation was also calculated using Equation 7, basing the value of *h* on Lunardini *et al.* (1986). *h* is commonly related to the Nusselt number (Nu) based on the hydraulic radius (R_h), using the formula $h = \frac{Nu.k_w}{R_h}$, where k_w [$W.m^{-1}.°C^{-1}$] is the thermal conductivity of water. The Nusselt number is computed for each value of the Reynolds number ($Re = \frac{\rho_w.R_h.V_w}{\eta_w}$, where ρ_w [$kg.m^{-3}$] is the density of water, V_w [$m.s^{-1}$] is the average water velocity and η_w [Pa.s] is the dynamic viscosity of water) and Prandtl number ($Pr = \frac{\eta_w.c_{pw}}{k_w}$, where cp_w [$J.kg^{-1}.°C^{-1}$] is the specific heat of water), through the previously

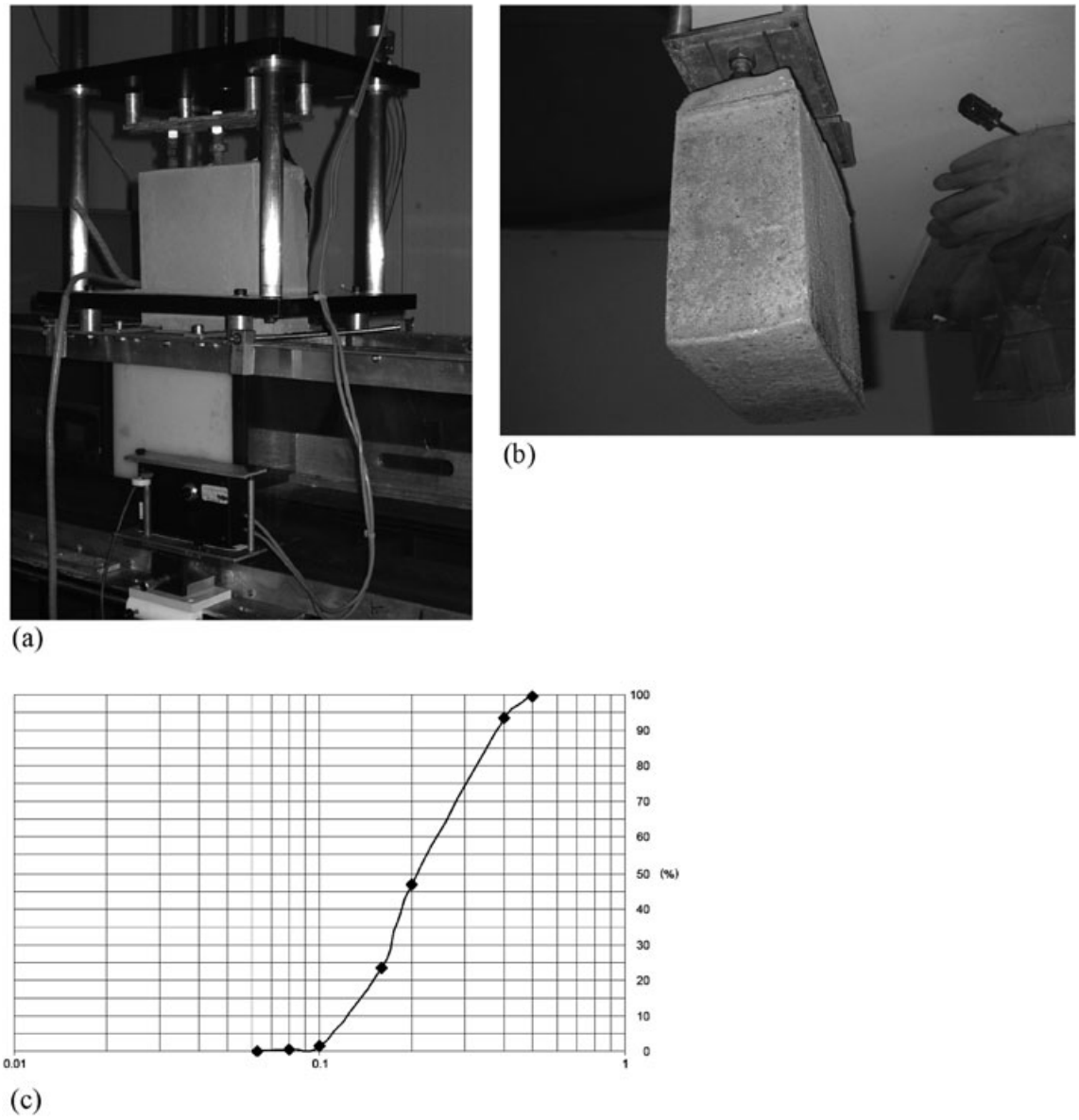

Figure 2 Laboratory experimental setup. (a) The frozen sample is placed in the moving track and is lowered until its surface reaches the flowing water and then erosion begins. (b) Sample removed from the track after the experiment showing a regular erosion surface. (c) Grain size distribution of Bayeux sand is virtually identical to sands from the banks of the Lena River.

determined empirical relation: $Nu = 0.00249.Pr^{1/3}.Re^{1.0552}$ (Randriamazaoro, 2007).

RESULTS

Effects of Ice Content on the Ablation Rate

Measurements of ablation rates for sandy samples with differing ice contents were made for a Reynolds number equal to 15 900, corresponding to a turbulent flow regime with an average velocity V_w of 0.188 m s^{-1}, a water temperature of 5.5 °C and an initial sample temperature of −7 °C. Measurements for pure ice and permafrost with ice contents of 80% and 20% are in good agreement with the ablation model (Figure 3). The model predicts an ablation rate that increases as the ice content decreases, with values of 0.7 mm min^{-1}, 0.9 mm min^{-1} and 1.7 mm min^{-1} for pure ice, 80% ice contents and 20% ice contents, respectively. The highest degree of linearity was obtained experimentally for pure ice while slight fluctuations of the measured erosion rate around the predicted values were observed for the frozen sediments (Figure 3). These fluctuations were greater for lower ice contents and related to the accumulation of thawed sand grains. At ice contents lower than saturation ($\omega < 20\%$), the model of pure ablation

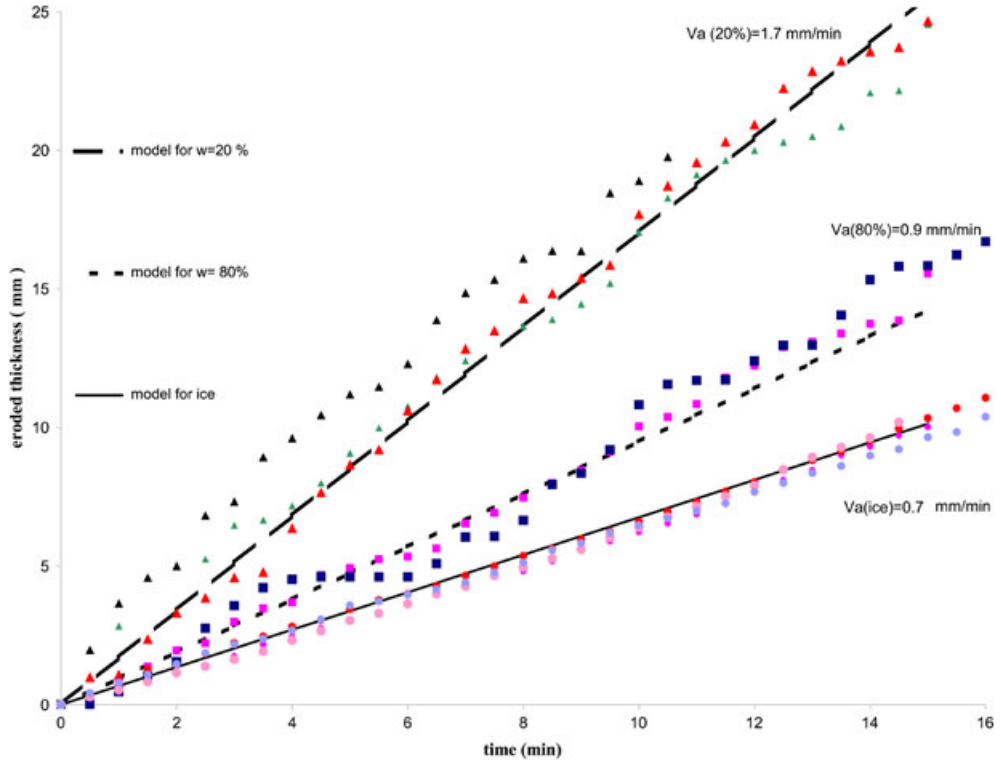

Figure 3 Eroded thickness through time for a sandy frozen sample with different ice contents (ω) (pure ice, ω = 80% and ω = 20%). The measured values in repeated experiments are compared with the values predicted by the ablation model for the same parameters. The water temperature was 5.5 °C, the Reynolds number 15 900 and the initial sample temperature −7 °C. Va = ablation rate.

cannot be applied because mechanical aspects can no longer be neglected.

Another series of experiments was undertaken with a Reynolds number of 12 700, corresponding to an average flow velocity of 0.150 m s^{-1}. The pure ice sample was again eroded less than the frozen sample with 80% ice content (Figure 4a). In addition, the ablation model for 80% ice content predicted an ablation rate of 0.66 mm min^{-1}, while the best-fit linear regressions for three experiments gave 0.61 mm min^{-1}, 0.58 mm min^{-1} and 0.57 mm min^{-1}. On average, therefore, the pure ablation model over-predicted the erosion rate by 11%. Experiments on a sample with 20% ice content, however, showed that this was beyond the limit of validity of the ablation model because the measured erosion rates were half those predicted (Figure 4b).

Critical Ice Content

The experiments suggest that above a critical ice content thawed sediments are so easily washed away by the flow that a model of pure ablation can adequately represent the entire process. Below this critical ice content, the pure ablation model over-predicts the erosion rate as the removal of sediments no longer occurs immediately following thaw. This critical ice content depends on the dynamics of the turbulent flow. For Reynolds number 15 900, the measured erosion rate and the theoretical ablation rate are virtually the same for ice contents greater than 20%. For Reynolds number 12 700, the ablation model slightly over-predicts the real erosion rates for high ice contents (80%) and greatly over-predicts for lower ice contents (20%). Therefore these two sets of experiments indicate that the critical ice content is around 80% for Reynolds number 12 700 (0.15 m s^{-1}) and 20% for Reynolds number 15 900 (0.19 m s^{-1}).

Process of Thermal Erosion Below the Critical Ice Content

A more detailed examination of the measured eroded thickness for a critical case (Figure 4a, ω = 80%, Re = 12 700) suggests that erosion alternates between two phases. The first typically lasts a few minutes and is characterised by an erosion rate equal to the theoretical ablation rate. During the generally brief (typically ~1 min) second phase, erosion slows down and sometimes stops. Given that the sample is non-cohesive sands, this is attributed to the imbrication of grains periodically resisting fluid entrainment. Because of the brief duration of this phase, the layer of unremoved sand is very thin, the thermal process is not affected and the subsequent ablation phase begins at the same rate.

It is difficult to estimate a theoretical erosion rate for this episodic process that alternates between pure ablation and pure thaw, but the minimum and maximum thickness of the

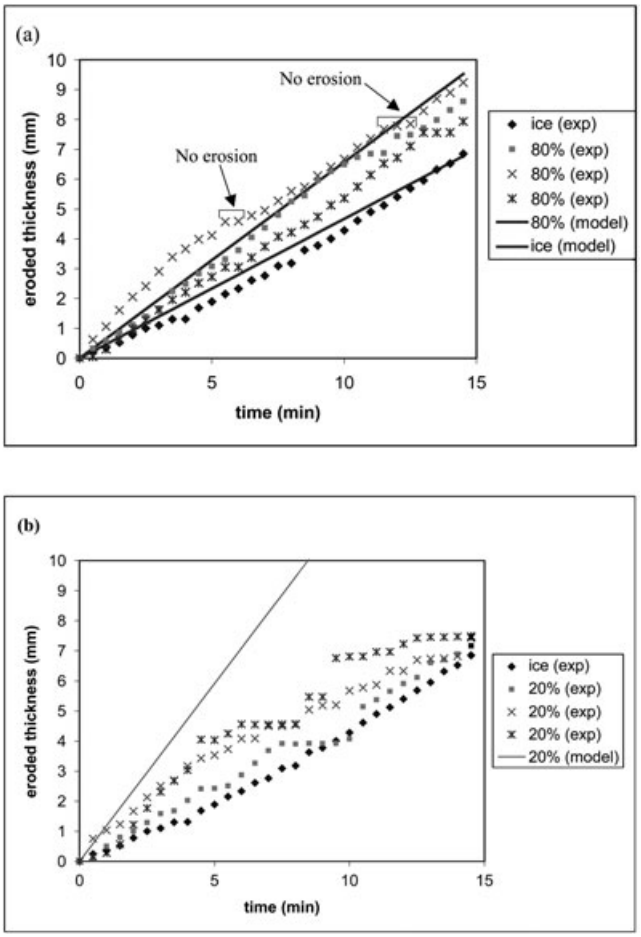

Figure 4 Eroded thickness through time for a sandy frozen sample with (a) 80% ice content and (b) 20% ice content. The water temperature was 5.5 °C, the Reynolds number 12 700 and the initial sample temperature −7 °C. The measured values in repeated experiments were compared with the values predicted by the ablation model for the same parameters. The ablation model predicts ablation velocities equal to 0.47 mm min^{-1} and 0.66 mm min^{-1} for ice and permafrost with 80% ice content, respectively.

thawed material (which in total includes the part removed by ablation) can be predicted by the pure thaw model and the pure ablation model, respectively. For example, a frozen sandy sample initially at −7 °C, with 20% ice content, subject to flowing water at 5.5 °C with a Reynolds number equal to 12 700 (Figure 4b) shows phases of ablation alternating with phases of thaw. After 10 min, the thawed material should theoretically be between 4 mm thick if not removed and 12 mm thick if removed (Figure 4b). The laboratory measurements gave an eroded thickness equal to 6 mm after 10 min, thereby providing an empirical minimum value for the thawed layer's thickness.

DISCUSSION AND CONCLUSIONS

The proposed model of thermal erosion applies to river banks developed in perennially frozen non-cohesive sediments. Above a critical ice content, an ablation model with instantaneous removal of thawed sediments can be applied, while below this ice content, a process of thermo-mechanical erosion occurs in which mechanical entrainment may be deferred.

The ablation model predicts erosion rates for ice contents of 80%, 40% and 20% of about one-and-a half times, two times and three times those for pure ice, irrespective of water flow characteristics (temperature and discharge). These results were validated experimentally for sandy frozen samples with ice contents of 20% and 80%. The effects of sediment temperature are small for pure ice (Costard *et al.*, 2003) and also appear to be small for high ice-content frozen soils. At low ice contents (close to saturation), however, the effects of ground temperature and ice content may be of a similar order of magnitude. As an example, an erosion rate twice that of pure ice at 0 °C is predicted for frozen sediment at 0 °C with a 35% ice content or at −40 °C with a 20% ice content. The same increase in ablation rate can be obtained by raising the water temperature from 1 °C to 2 °C. This example demonstrates that the main parameter in the thermal erosion process is

water temperature and that the ice content effect usually exceeds that of the ground temperature effect since the range of ground temperature variations during spring melt is typically less than 10 °C.

A critical ice content was inferred that depends on the Reynolds number of flowing water. Above this critical ice content, the mechanical removal of sediments occurs as soon as the ground ice melts and the model of instantaneous ablation is valid. At a Reynolds number of 15 900, the critical ice content is close to saturation (~20%) while for Reynolds number 12 700, it is around 80%. Our results are consistent with the predictions of Are (1983) who noted that the coast recedes continuously when ice content exceeds porosity.

Below the critical ice content, the flow may not be powerful enough to entrain the thawed sediments. The experiments show fluctuations around the theoretical values of the ablation model, which are explained by the non-removal of thawed sand grains. If the ice content is decreased further, the average measured erosion rates fall far below the predicted ablation rate. Similarly, in the field, calculated ablation rates usually greatly exceed observed coastal erosion rates because modelling assumes mechanical erosion of the thawed sediments (Are, 1983). The laboratory experiments show the alternation of periods of ablation of a few minutes' duration with briefer periods (~1 min) of stabilisation of sand grains at the water/frozen sediment interface. The latter is interpreted as the effect of imbrication of sandy grains due to the heterogeneous and non-spherical distribution of sand in the laboratory samples.

Our classification concerning the response of non-cohesive material to pure ablation and thermo-mechanical erosion may explain apparently contradictory field observations. In some parts of the Lena River banks, ice-rich layers protrude by a few decimetres compared to the surrounding sandy permafrost layers, which typically have 20% ice content (Figure 1). These banks were subject to high discharges (50 000 $m^3.s^{-1}$ during the flood season), which favour an ablation process and faster erosion for lower ice contents as explained by this study. Elsewhere, however, and as frequently reported in the literature, the greatest erosion occurs in permafrost with the highest ice contents. In many cases, this appears to be because the material is cohesive and erosion characteristics of non-cohesive sediments change greatly when small amounts of clay (between 3% and 15% clay content for the transition) are present (Mitchener and Torfs, 1996). This study applies to sandy permafrost and clearly explains the combined effects of ice content and water flow on the thermal erosion process.

ACKNOWLEDGEMENTS

We appreciate the thoughtful review of two anonymous reviewers. We thank Laurence Jouniaux and Mattew Balm for constructive discussions. These investigations were supported by the GDR 'mutations polaires: société et environnement', the 'Programme RELIEFS' from the Institut National des Sciences de l'Univers (CNRS, France) and the Agence Nationale de la Recherche (ANR-07-VULN 002 CLIMAFLU).

REFERENCES

Aberle J, Nikora V, Walters R. 2004. Effects of bed material properties on cohesive sediment erosion. *Marine Geology* **207**: 83–93.

Aguirre Puente J, Costard F, Posado-Cano R. 1994. Contribution to the study of thermal erosion on Mars. *Journal of Geophysical Research* **99** (3): 5657–5667.

Are FE. 1983. Thermal abrasion of coasts. In *Proceedings of the 4th International Conference on Permafrost*, 18–22 July 1983, Washington D.C., National Academy Press: Fairbanks, Alaska. 24–28.

Carslaw HS, Jaeger JC. 1959. *Conduction of Heat in Solids*. Oxford Science Publication: New York; 510pp.

Costard F, Gautier E. 2007. The Lena River: main hydromorphodynamic features in a deep permafrost zone. In *Large Rivers: Geomorphology and Management*, Gupta A (ed). John Wiley & Sons: Chichester, England; 225–232.

Costard F, Dupeyrat L, Gautier E, Carey-Gailhardis E. 2003. Fluvial thermal erosion investigations along a rapidly eroding river bank: Application to the Lena river (Central Siberia). *Earth Surface Processes and Landforms* **28**: 1349–1359.

Couper P. 2003. Effects of silt-clay content on the susceptibility of river banks to subaerial erosion. *Geomorphology* **56**: 95–108.

Dysli M. 2003. Scaling of supersaturation by a simple test. In *Permafrost*, Philips, Springman and Arenson (eds). Swets & Zeitlinger: Lisse; 223–227.

Farouki OT. 1981. Thermal properties of soils. Special Report 81–1. Cold Regions Research and Engineering Laboratory (CRREL), Hanover, NH.

Fukuda MK, Lick W. 1980. The entrainment of cohesive sediments in freshwater. *Journal of Geophysical Research* **85**(C5): 2813–2824.

Gatto LW. 1995. Soil freeze-thaw effects on bank erodibility and stability. Special Report 95–24. Cold Regions Research and Engineering Laboratory (CRREL), Hanover, NH.

Gautier E, Costard F. 2000. Les systèmes fluviaux à chenaux anastomosés en milieu périglaciaire : la Léna et ses principaux affluents (Sibérie centrale). *Géographie physique et quaternaire* **54**(3): 327–342.

Gillie RD. 1990. Beaufort sea artificial island erosion data. Environmental Studies Revolving Funds, Report No. 096, Ottawa, 1988.

Héquette A, Barnes PW. 1990. Coastal retreat and shoreface profile variations in the Canadian Beaufort sea. *Marine Geology* **91**: 113–132.

Hoque MA, Pollard WH. 2005. Modeling block failures in vertical cliffs of Arctic coasts underlain by permafrost. In *Proceedings of the 5th International Workshop of Arctic Coastal Dynamics*, McGill University, Montreal (Canada), 13–16 October 2004, Rachold V, Lantuit H, Couture N, Pollard W (eds). Berichte zur Polar- und Meeresforschung = Reports on Polar and Marine Research, Alfred-Wegener-Institut für Polar- und Meeresforschung: Bremerhaven, Federal Republic of Germany; **506**: 60–64.

Jepsen R, Roberts J, Lick W. 1997. Effects of sediment bulk density on sediment erosion rate. *Water Air and Soil Pollution* **99**: 21–37.

Johansen O. 1975. Thermal conductivity of soils. PhD thesis, Trondheim, Norway, 236pp.

Kobayashi N. 1985. Formation of thermoerosional niches into frozen bluffs due to storm surges on the Beaufort Sea Coast. *Journal of Geophysical Research* **90**(C6): 11983–11988.

Kobayashi N, Vidrine JC, Nairn RB, Solomon S. 1999. Erosion of frozen cliffs due to storm

surge on Beaufort Sea Coast. *Journal of Coastal Research* **15**(2): 332–344.

Lantuit H, Overduin PP, Couture N, Odegard RS. 2008. Sensitivity of coastal erosion to ground ice content: An arctic-wide study based on the ACD classification of arctic coasts. In *Proceedings of the 9th International Conference on Permafrost*, DL Kane, KM Hinkel (eds). Institute of Northern Engineering University of Alaska Fairbanks: 1025–1029.

Lawler DM, Thorne CR, Hooke JM. 1997. Bank erosion and stability. In *Applied Fluvial Geomorphology for River Engineering and Management*, Thorne CR, Hey RD, Newson MD (eds). John Wiley & Sons: Chichester; 137–172.

Lick W, McNeil J. 2001. Effects of sediment bulk properties on erosion rates. *The Science of the Total Environment* **266**: 41–48.

Lunardini VJ, Zisson JR, Yuen YC. 1986. Experimental determination of heat transfer coefficients in water flowing an horizontal ice sheet. Special Report 3–86. Cold Regions Research and Engineering Laboratory (CRREL), Hanover, NH.

Mitchener H, Torfs H. 1996. Erosion of mud/sand mixtures. *Coastal Engineering* **29**: 1–25.

Ogorodov SA. 2008. Effects of changing climate and sea ice extent on Pechora and Kara seas coastal dynamics. In *Proceedings of the 9th International Conference on Permafrost*, DL Kane, KM Hinkel (eds). Thomas Alton and Fran Pedersen, Institute of Northern Engineering University of Alaska Fairbanks: 1317–1320.

Osman AM, Thorne CR. 1988. Riverbank stability analysis I: Theory. *Journal of Hydraulic Engineering* **114**: 134–150.

Randriamazaoro R. 2007. Modélisation numérique et analogique de l'érosion thermique. PhD thesis, Université Paris XI, France, 209pp.

Randriamazaoro R, Dupeyrat L, Costard F, Carey Gailhardis E. 2007. Fluvial thermal erosion: heat balance integral method. *Earth Surface Processes and Landforms* **32**: 1828–1840.

Roberts J, Jepsen R, Gotthard D, Lick W. 1998. Effects of particle size and bulk density on erosion of quartz materials. *Journal of Hydraulic Engineering* **124**(12): 1261–1267.

Scott KM. 1978. Effects of permafrost on stream channel behaviour in Arctic Alaska. US Geological Survey Professional Paper 1068.

Soloviev PA. 1962. Alas relief and its origin in Central Yakuta, Many years permafrost associated with their phenomenum in Yakutz. In *Mnogoletnemerzlye porody i soputsvuscie im yavleniya na territorii.* JASSR, Izdatelstvo AN SSSR, Moscow (1962), 38–53.

Thorne CR, Tovey NK. 1981. Stability of composite river banks. *Earth Surface Processes and Landform* **6**: 469–484.

Van Everdingen R (ed). 1998 revised 2005. *Multi-language glossary of permafrost and related ground ice terms*. Boulder, CO: national Snow and Ice data Center/World Data Center of Glaciology.

Walker HJ. 1983. Erosion in a permafrost-dominated delta. In *Proceedings of the 4th International Conference on Permafrost*, 18–22 July 1983. National Academy Press, Washington DC: Fairbanks, Alaska. 1344–1349.